Supporting Information

Multiple Promotion Effect of Mixed Solvents on Oxidative Degradation of Thermosetting Polymers

Yuwei Long, Zhishan Su, Lan Bai, Xu Zhao, Wenli An, Xuehui Liu Shimei Xu*, Yu-Zhong Wang*

Table of Contents

Computational details

The cross-linked epoxy polymer was constructed using the diglycidyl ether of bisphenol A (DGEBA) and 4,4'-diaminodiphenylmethane (DDM) as epoxy monomers and cross-linkers, respectively. 60 DGEBA and 20 DDM were crosslinked into the epoxy polymer by using the Amorphous module of Material studio, with a crosslinked degree of 100%.

The molecular dynamics (MD) simulation was performed using the GROMACS 2018.8 software[1], with periodic boundary condition. For the dry polymer, successive annealing cycles were run and NPT ensemble was selected for a duration of 10 ns to reach an equilibrium state under isothermal and pressure conditions. The structures of three organic solvents (i.e., DMF, CH_3CN and THF) were optimized at the M062X-D3/6-31G(d,p)[2-4] level of theory using Gaussian 09 program package[5]. The corresponding restrained electrostatic potential (RESP) charge were calculated by the Multiwfn software[6-7]. Packmol program[8] was used to construct a suitable solvent box, and NPT ensemble was selected to obtain a reasonable density at 298 K and 1 bar pressure (Table S7). The swelling model with cross-linked epoxy polymer and solvents in the box (Figure S20) was pre-equilibrated for 5 ns in the NPzT ensemble, followed by a 50 ns NVT production simulation under the same condition. GAFF force field[9] was adopted to describe the epoxy polymer and organic solvents, whereas the water was described by SPC/E model[10]. Nosé-Hoover thermostat was used to control the temperature, and the pressure was controlled by the Berndsen in a semi-isotropic manner to reach equilibrium state.

A box containing one organic molecule and 1000 water molecules was built by Packmol program (Figure S21). After the minimization simulation, the NVT ensemble for 5 ns was carried out under 298 K and 1 bar to reach the equilibrium state. The trajectory of the last 1ns, which was fully 1000 frames, was taken to study the interaction between organic molecule (i.e., DMF, CH3CN, and THF) and water cluster by averaged RDG (aRDG) method[11] in Multiwfn software. The thermal fluctuation index(TFI) was visualized to evaluate the stability of the weak interaction in different regions. In the simulation, the organic molecule was frozen to ensure adequate contact with the water.
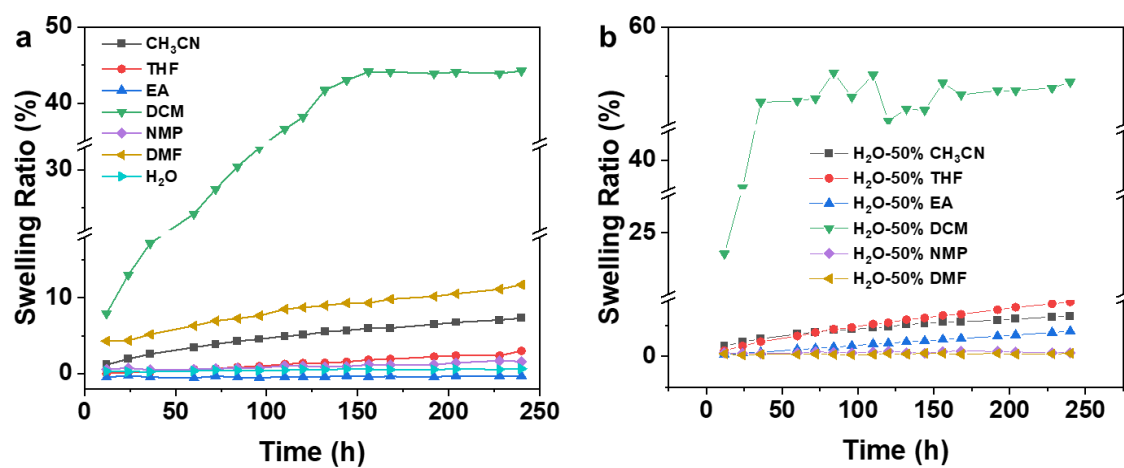
Results and Discussion

Figure S1. Swelling of EP by different solvents (a. different single solvents, b. different mixed solvents).
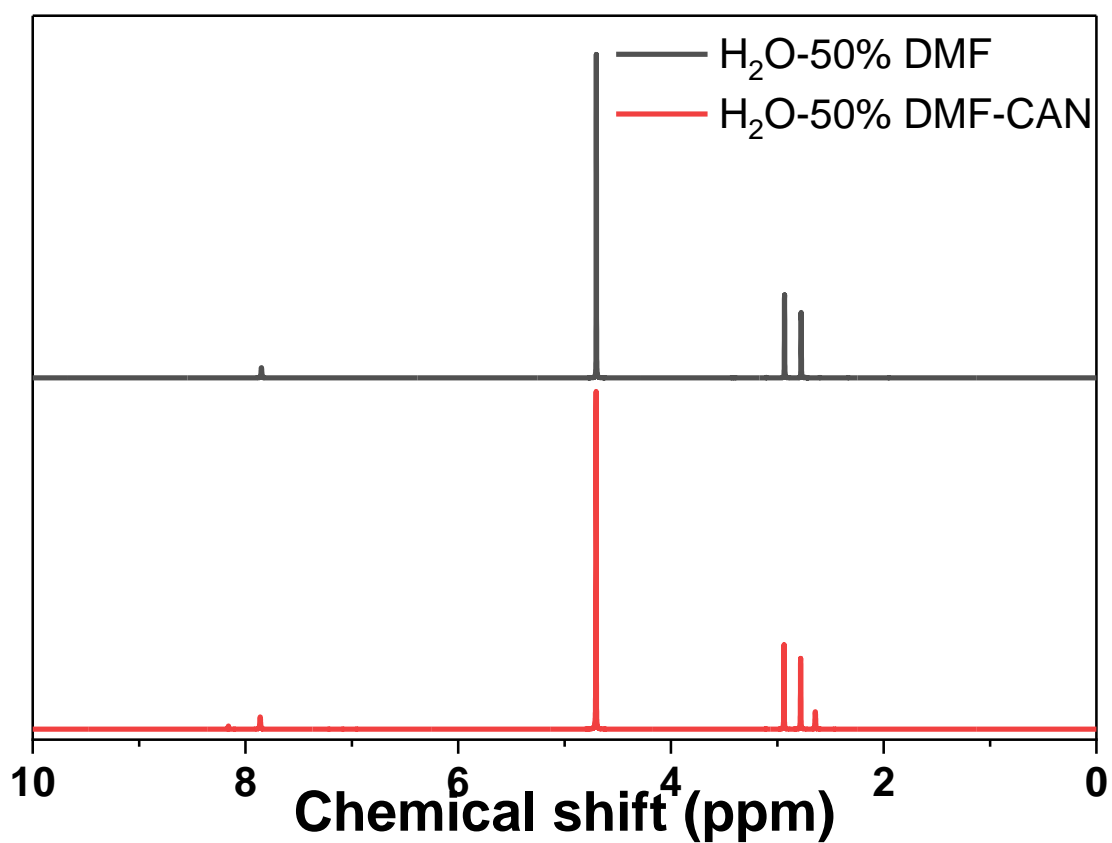
Figure S2. The NMR spectra of H_2O -50% DMF and H_2O -50% DMF with CAN.

However, there was no difference between NMP-50% H2O solutions with and without CAN. The integrated peak ratio of NMP is consistent with its stoichiometry ratio. It is further confirmed that NMP does not react with CAN. When NMP was added to the aqueous solution of CAN, the color of the solution was significantly deepened, and solids were precipitated. It is speculated that NMP and water formed strong hydrogen bonds, which affected the dissolution of water to CAN, and the solubility of CAN in NMP was not good so that a large amount of CAN is precipitated. When the concentration of CAN decreases, and the reactivity is lower than that of the aqueous solution.
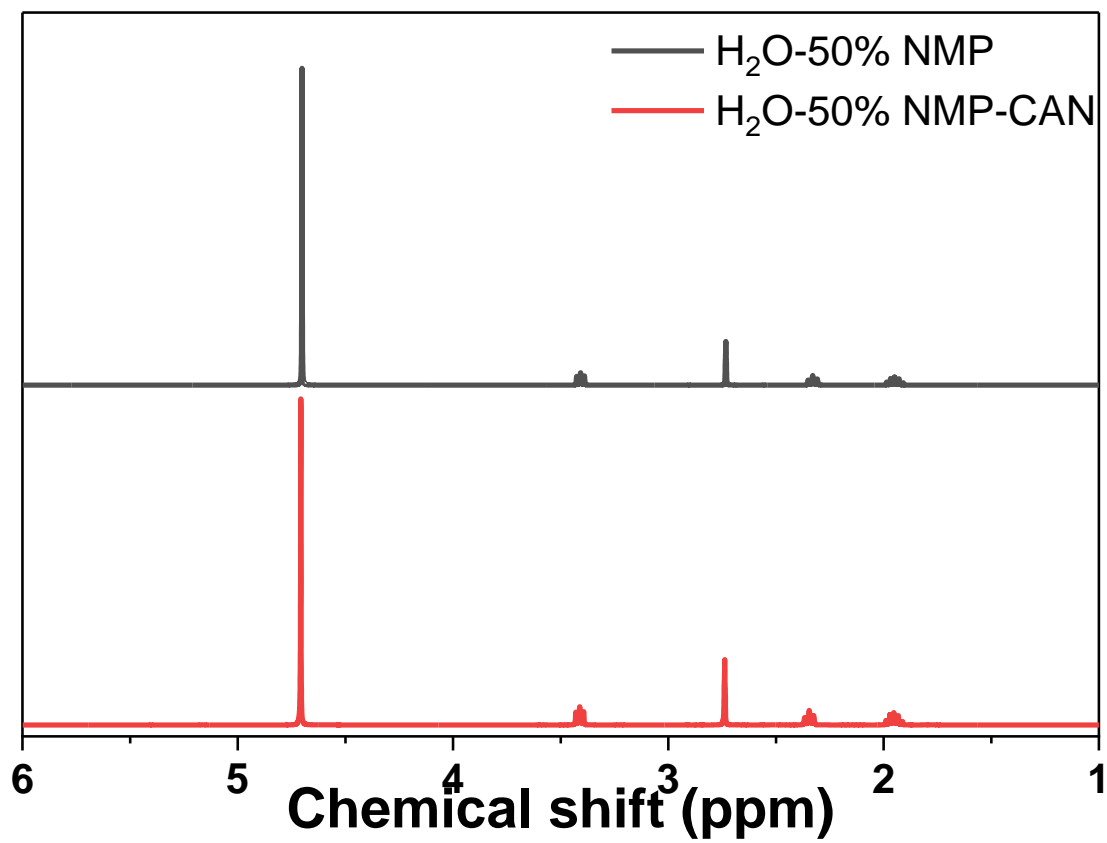
Figure S3. The NMR spectra of H_2O-50% NMP and H_2O-50% NMP with CAN.

Table S1. Solubility parameters of resins and different solvents.

| Sample	δt	δd	δp	δh	$\Delta\delta$	$(\Delta\delta t)^2$
H_2O	47.80	15.60	16.00	42.30	33.91	493.77
NMP	22.90	18.00	12.30	7.20	13.04	7.18
DMF	24.80	17.40	13.70	11.30	13.48	0.61
CH_2Cl_2	20.30	18.20	6.30	6.10	9.17	27.87
THF	19.40	16.80	5.70	8.00	8.41	38.18
EA	18.10	15.80	5.30	7.20	9.33	55.94
CH_3CN	24.40	15.30	18.00	6.10	19.30	1.39
H_2O-50%NMP	35.35	16.80	14.15	24.75	18.63	95.47
H_2O-50%DMF	36.30	16.50	14.85	26.80	20.58	114.94
H_2O-50%THF	33.60	16.20	10.85	25.15	17.01	64.34
H_2O-50%CH_3CN	36.10	15.45	17.00	24.20	20.80	110.69
DDM-E51	25.58	22.27	1.19	12.53	/	/
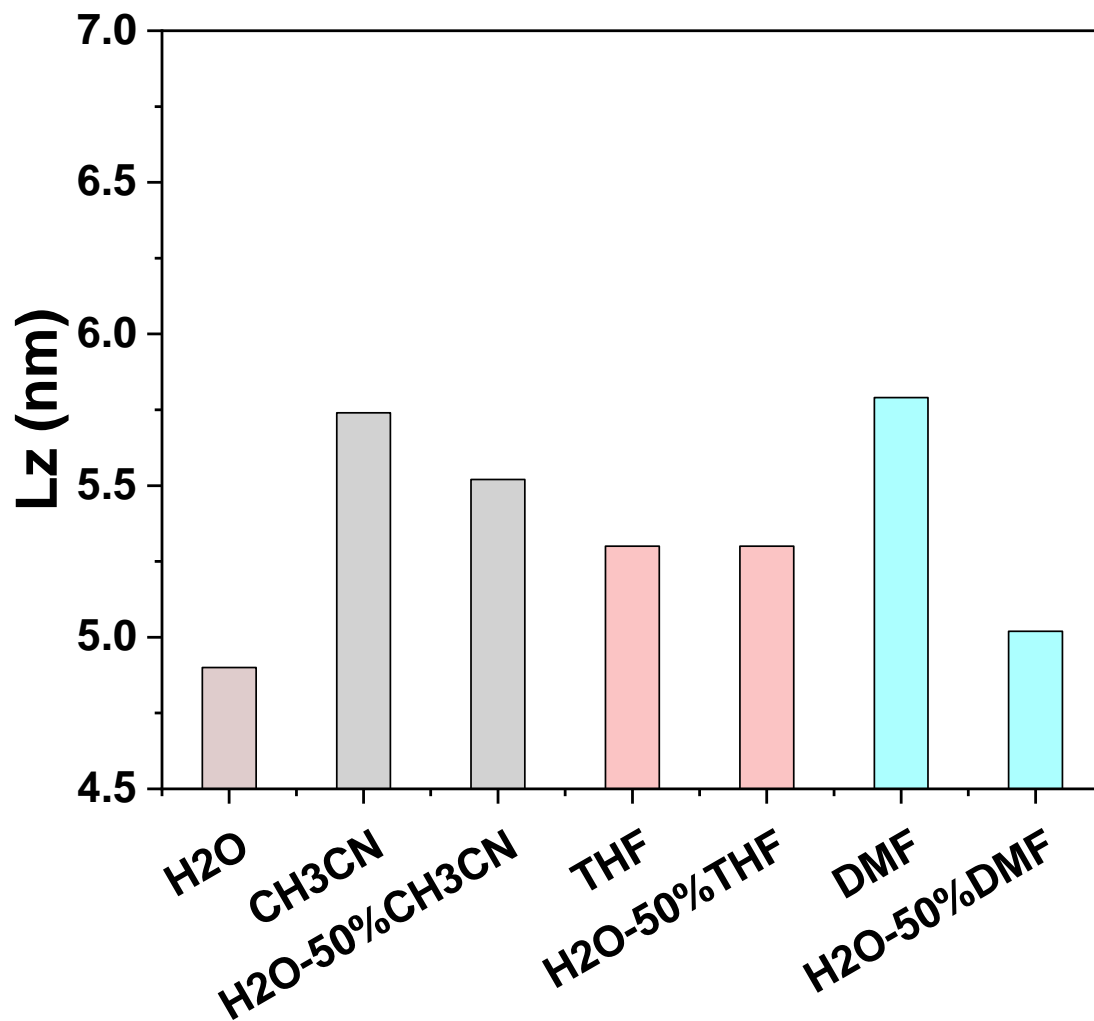
Figure S4. Length of polymers in different solvents along the z-axis (results of molecular dynamics simulations).
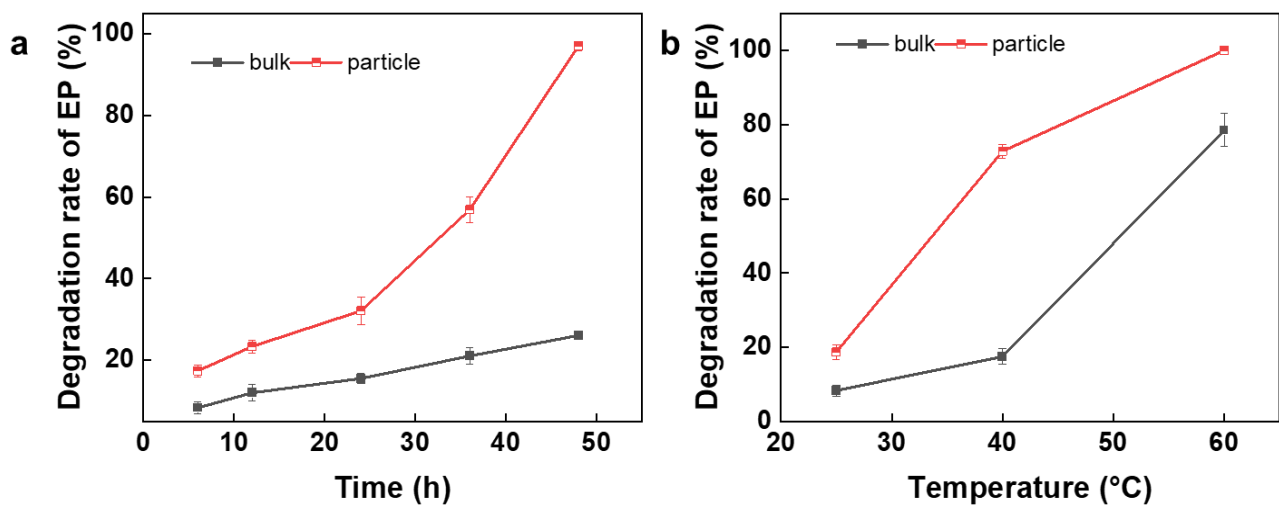
Figure S5. Degradation of EP by CAN H_2O-50%CH_3CN Solutions (a. Effect of reaction time on the degradation rate of resins with different sizes at 25°C (bulk resin: 10 mm*20 mm* 1mm, particle resin: 40 to 60 mesh), b. Effect of reaction temperature on the degradation rate of resins with different sizes for 6 h).

Table S2. The area of wetting color circles in Fig.4c.

Sample	Volume fraction of CH$_3$CN（%）	Area（μm²）
i	0	5531573
ii	25	6078498
iii	50	7341020
iv	75	7452940
v	80	7819137
vi	90	8067615
vii	100	8446212

Table S3 The degradation of EP in H_2O-50%CH_3CN solutions with and without DCM

Sample	Solvent	Temperature (°C)	Time (h)	Degradation rate (%)	Picture
1	H_2O-50%CH_3CN	40	6	100	
2	H_2O-50%CH_3CN-10%DCM	40	6	100	
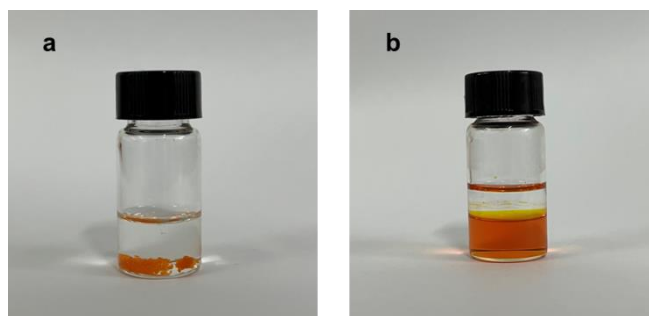
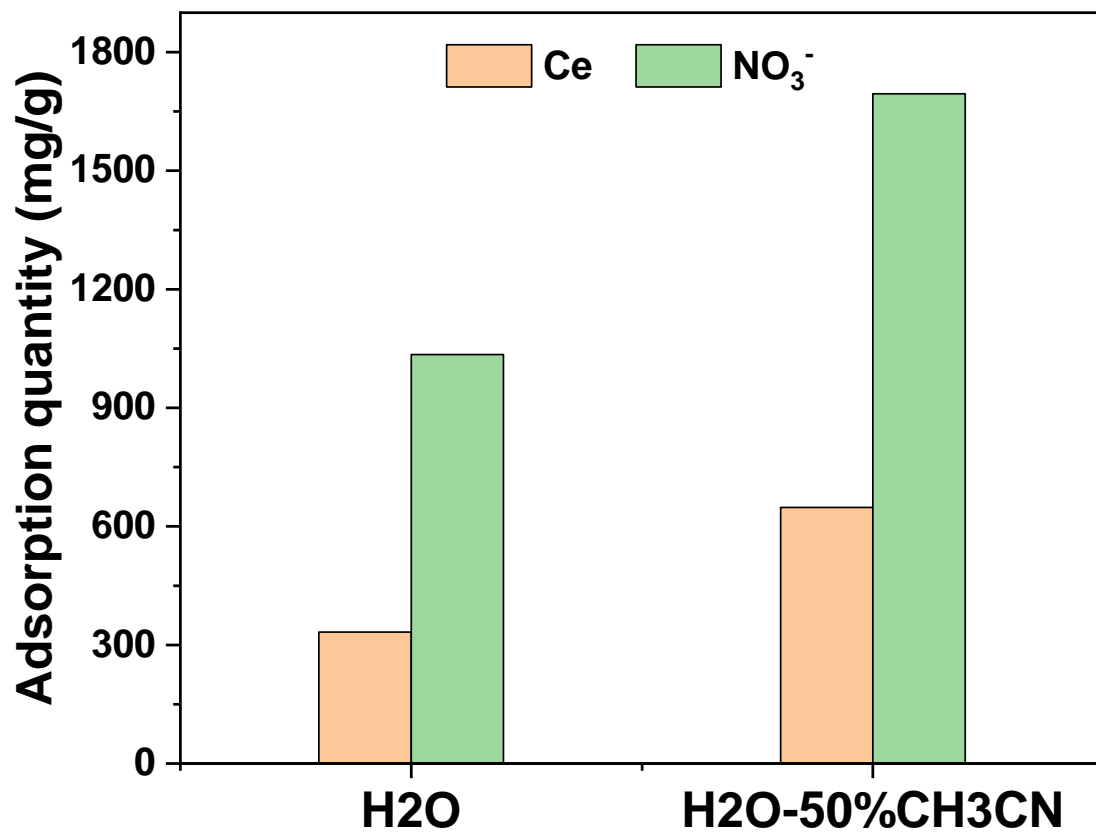**Figure S6** Photos of CAN-DCM(a) and CAN-DCM-H$_2$O(b)

Figure S7. Adsorption of Ce and NO_3^- by EP at 25°C for 6 h in different CAN solutions.
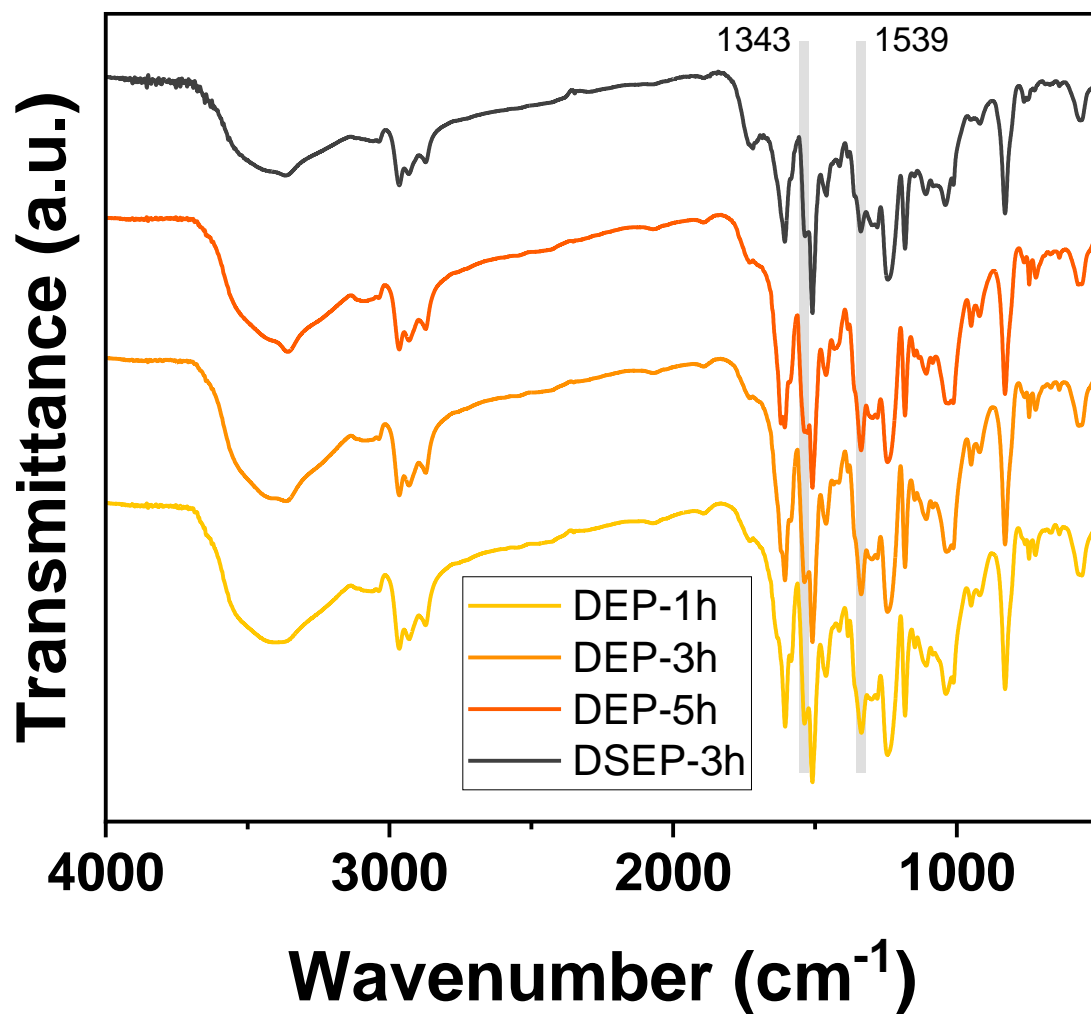
Figure S8. FTIR spectra of degradation products by different solvents (H_2O for DSEP, H_2O-50% CH_3CN for DEP) at 60°C in different degradation time.
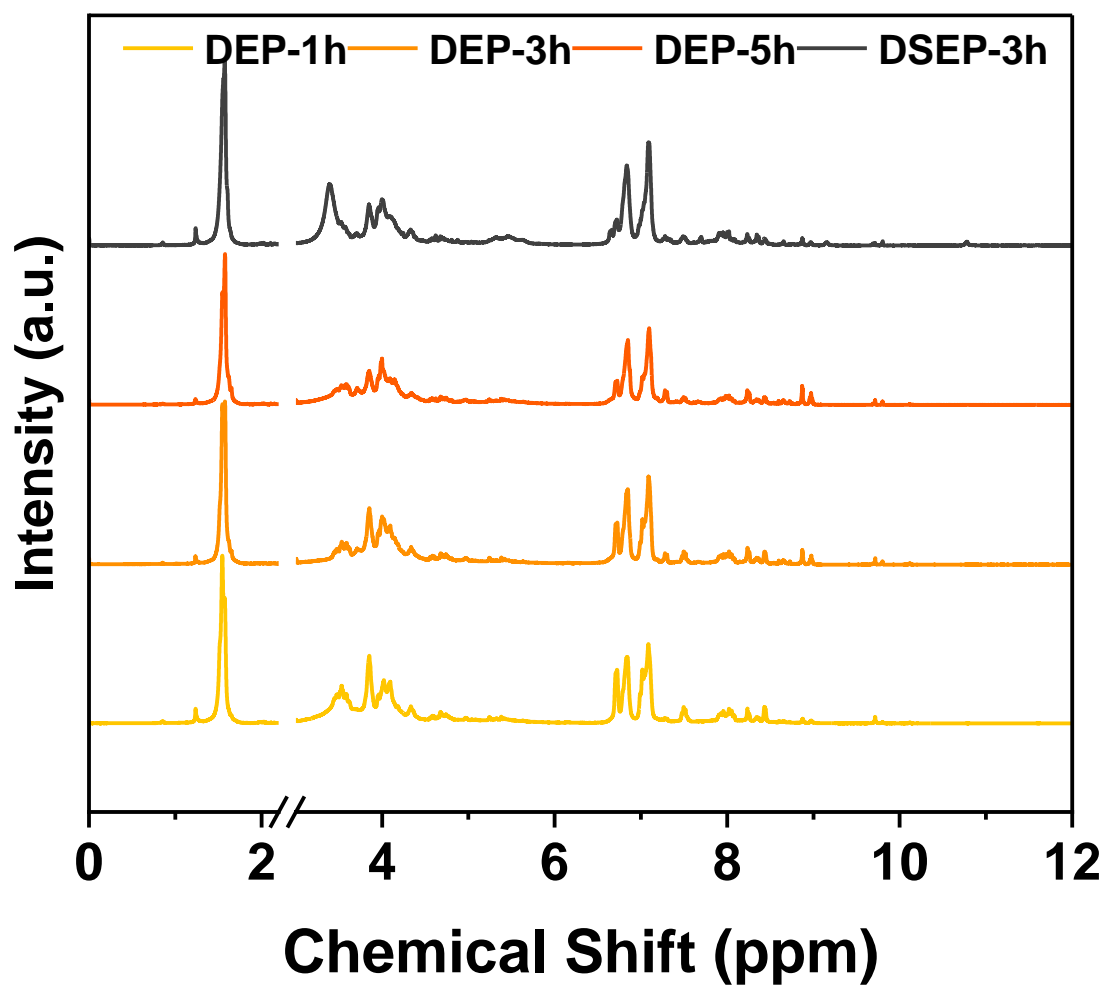
Figure S9. The ^{1}H-NMR spectra of degradation products by different solvents (H$_2$O for DSEP, H$_2$O-50% CH$_3$CN for DEP) at 60°C in different degradation time.
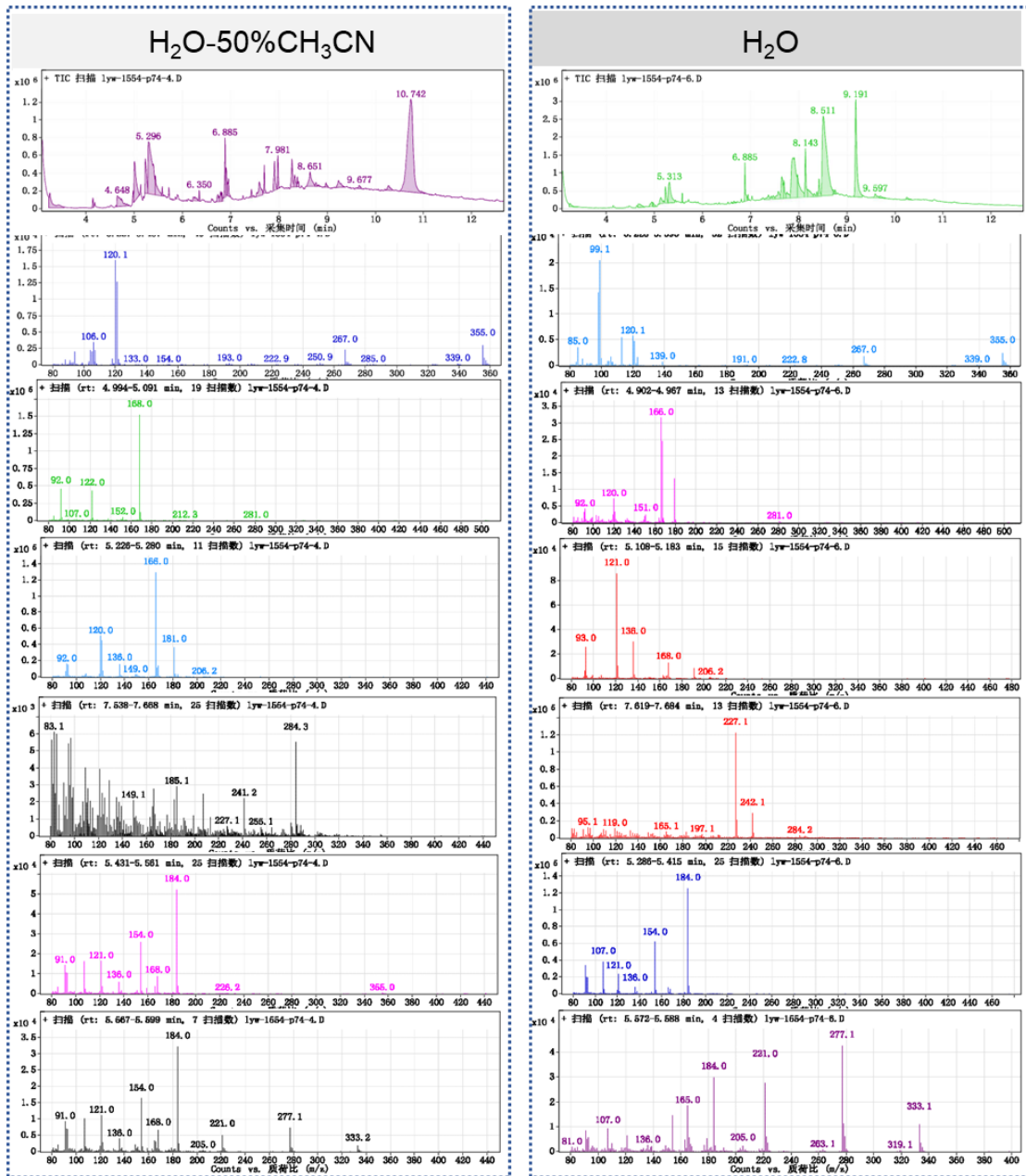
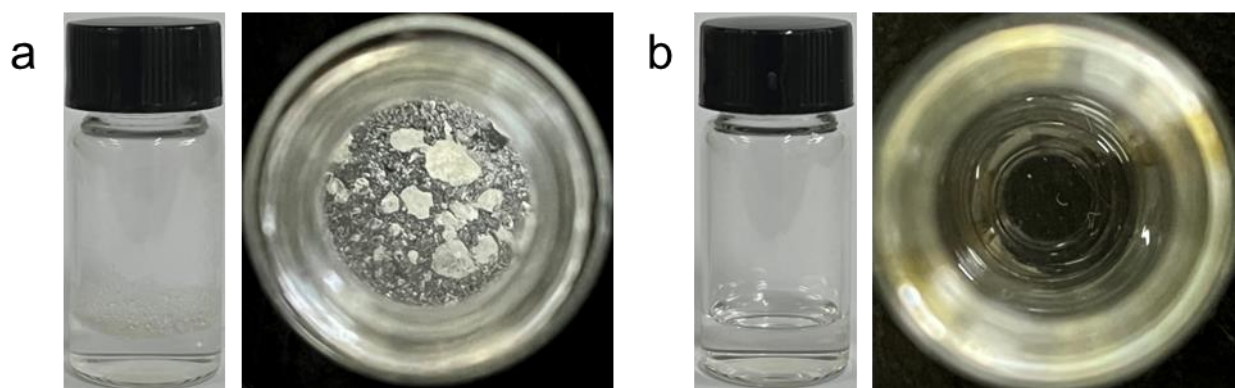**Figure S10**. GC-MS spectra of small molecular degradation products of EP in different solvents

16

Figure S11. Model compound in H_2O (a) and CH_3CN (b). The left side is the front view and the right side is the top view.

Model compounds prepared by the reaction of 4,4'-diaminodiphenylmethane with phenyl glycidyl ether, then the compound was degraded in CAN-H_2O and CAN-H_2O-50%CH_3CN respectively to investigate the effect of solvent on degradation. As shown in Figure S11, the model compound was insoluble in H_2O, whereas was completely dissolved in CH_3CN. Further GC-MS analysis of the degradation products in two kinds of solutions showed similar chromatograms peaks and the corresponding mass spectra were in general unity as the following Figure S12-14. Both the large molecule degradation products and the small molecule extracts are similar in both solutions. It is concluded that CH_3CN is not involved in the bond-breaking process and that the high-efficiency reaction is mainly attributed to the improved swelling of the resin and the increased oxidation of the oxidant at the presence of CH_3CN.
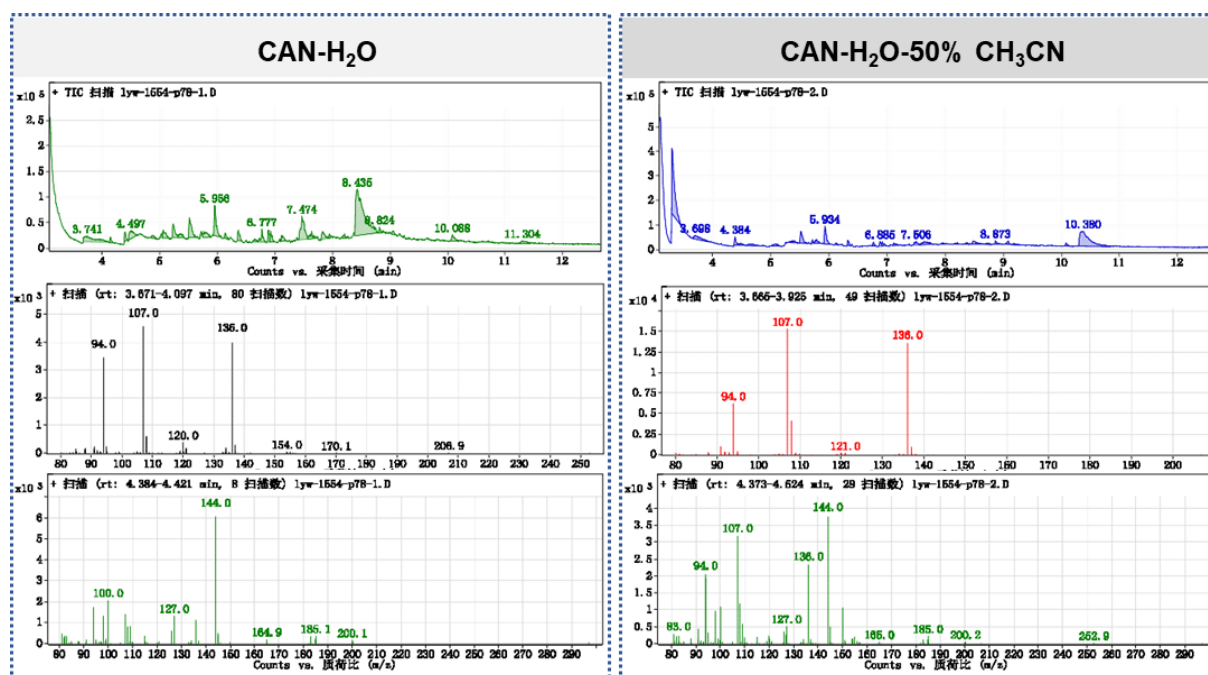

Figure S12. GC-MS spectra of degradation products of model compounds by CAN-H_2O and CAN-H_2O-50% CH_3CN respectively (rt:3.665-4.524)
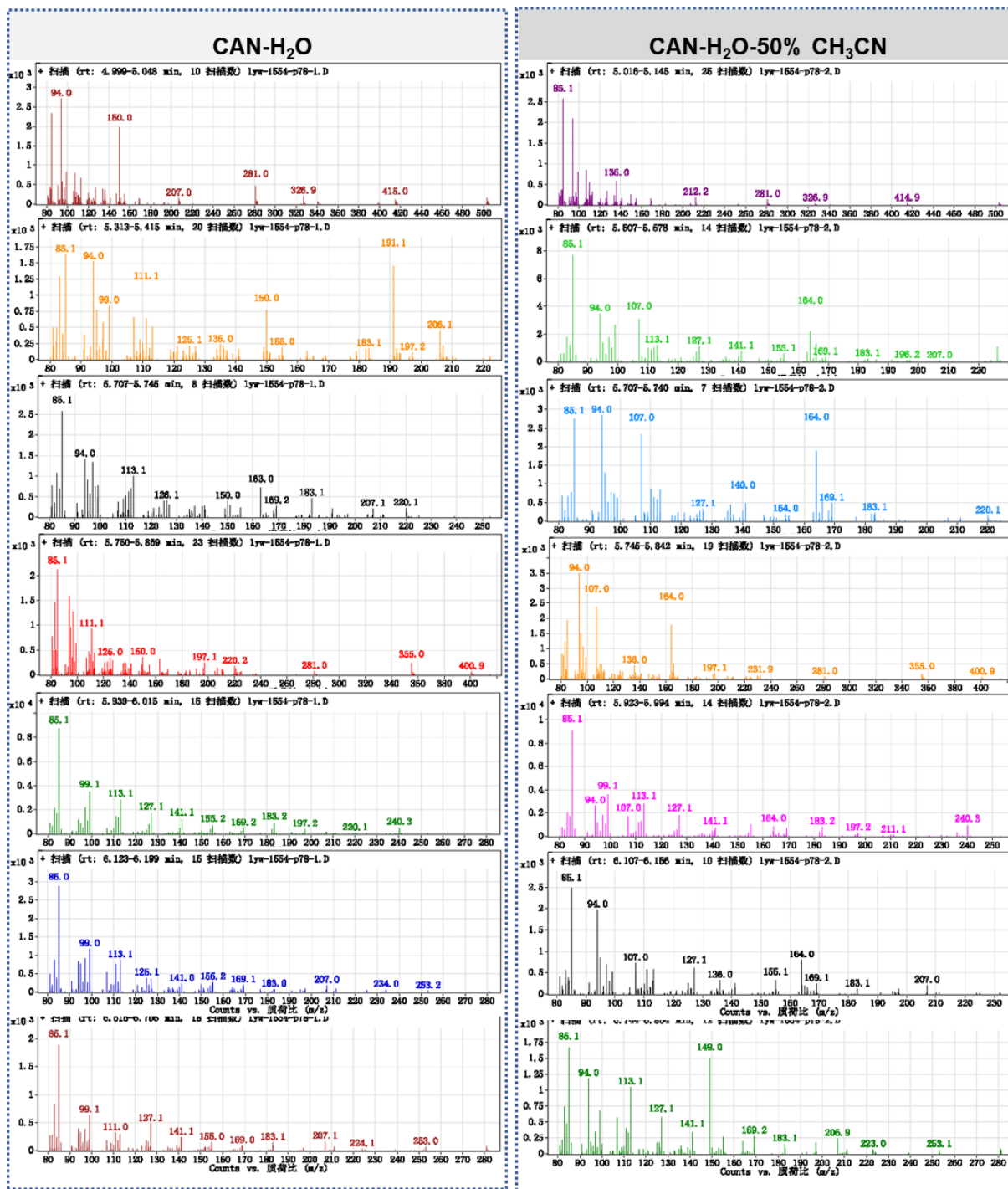
Figure S13. GC-MS spectra of degradation products of model compounds by CAN-H$_2$O and CAN-H$_2$O-50% CH$_3$CN respectively (rt:4.999-6.804)
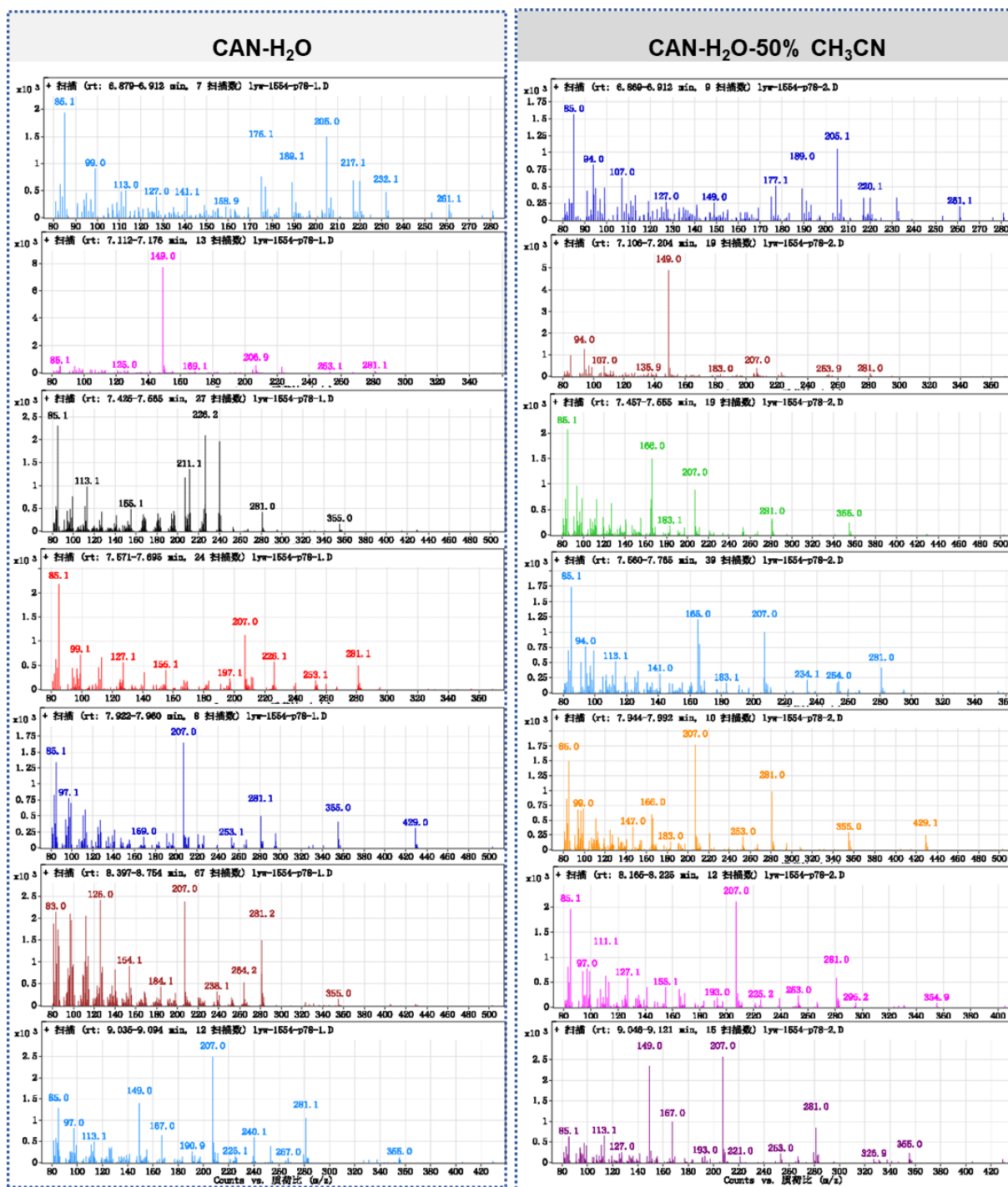
Figure S14. GC-MS spectra of degradation products of model compounds by CAN-H$_2$O and CAN-H2O-50% CH$_3$CN respectively (rt:6.869-9.121)

The absolute value of the reduction potential in H_2O-50%CH_3CN solution is lower than H_2O-50%THF but slightly higher than H_2O-50%DMF. No significant reduction peaks were observed in H_2O-50%NMP. This suggests that CAN is most easily reduced in DMF and CH_3CN, followed by THF and it is harder to be reduced in NMP. It agreed well with the experimental results except DMF in which a low degradation rate was observed. This may be attributed to poor mass transfer due to the low swelling rate of the resin in H_2O-50% DMF.
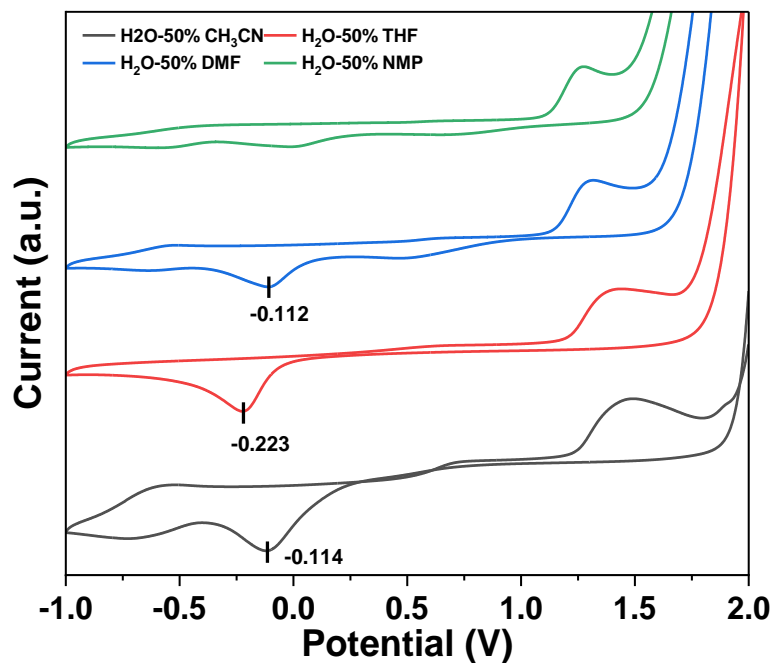

Figure S15. Cyclic voltammetry of CAN with different solvents

21

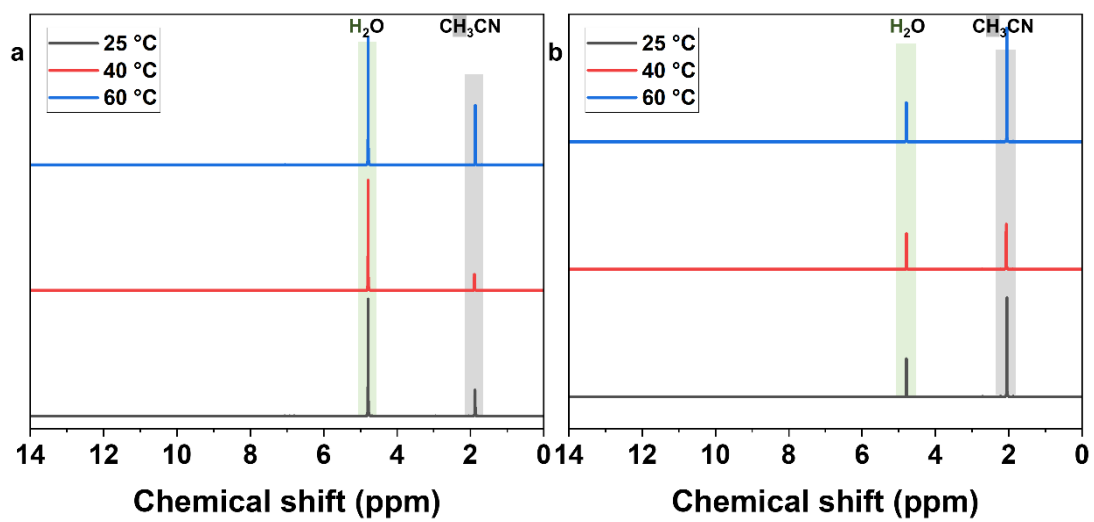**Figure S16.** NMR spectra of CH_3CN-H_2O at different temperatures (a)with and (b)without CAN

Table S4. The molecular weight and PDI of DEP at 60°C in different degradation time.

Sample	Mn	Mw	PDI
DEP-1h	1958	4981	2.54
DEP-3h	1811	4996	2.76
DEP-5h	1472	3626	2.46

Table S5. Elemental analysis of DEP at 60°C in different degradation time.

Sample	N(%)	C(%)	H(%)
DEP-1h	7.60	59.43	6.02
DEP-3h	7.68	58.40	5.39
DEP-5h	8.06	58.02	5.17

Sample	N(%)	C(%)	H(%)

Carbon fiber-reinforced epoxy composites (CFRP) are prepared using DDM as the curing agent and E51 as the epoxy monomer, through a hand lay-up process followed by hot-pressing procedure. Degradation of CFRP was carried out according to the degradation procedure of EP. After degradation, carbon fibers were washed by DMSO, then H_2O, and finally dried in a vacuum oven at 80ºC. Compared to pure water as solvent, the mixed solvent showed outstanding fast degradation speed. In an aqueous solution of 1.75M CAN, the clean fibers could not be obtained at 60 °C for even 10 h, whereas in a solution of CAN-H_2O-50%CH_3CN, the clean fibers were obtained after only 3 h of degradation. The SEM images show that the fibers were stripped from the composite through resin degradation, and the clean surface of the recovered fibers was similar to the virgin fibers, and the EDS results further verified that the recovered fibers have the same composition as the original fibers, with the main component being C. The fiber-reinforced composite degraded faster than the same size (2.5 mm*2.5 mm*10 mm) of pure resin bulk (Table S6). In this case, the inert carbon fibers in the composite did not participate in the reaction, but dispersed the resin, which facilitated the degradation reaction. In addition, the volume ratio of degradation liquid to the solid feedstock was fixed in the degradation experiments. So the resin content in the composite with the same size is lower than that of the pure resin bulk, which may also be more conducive to composite degradation.
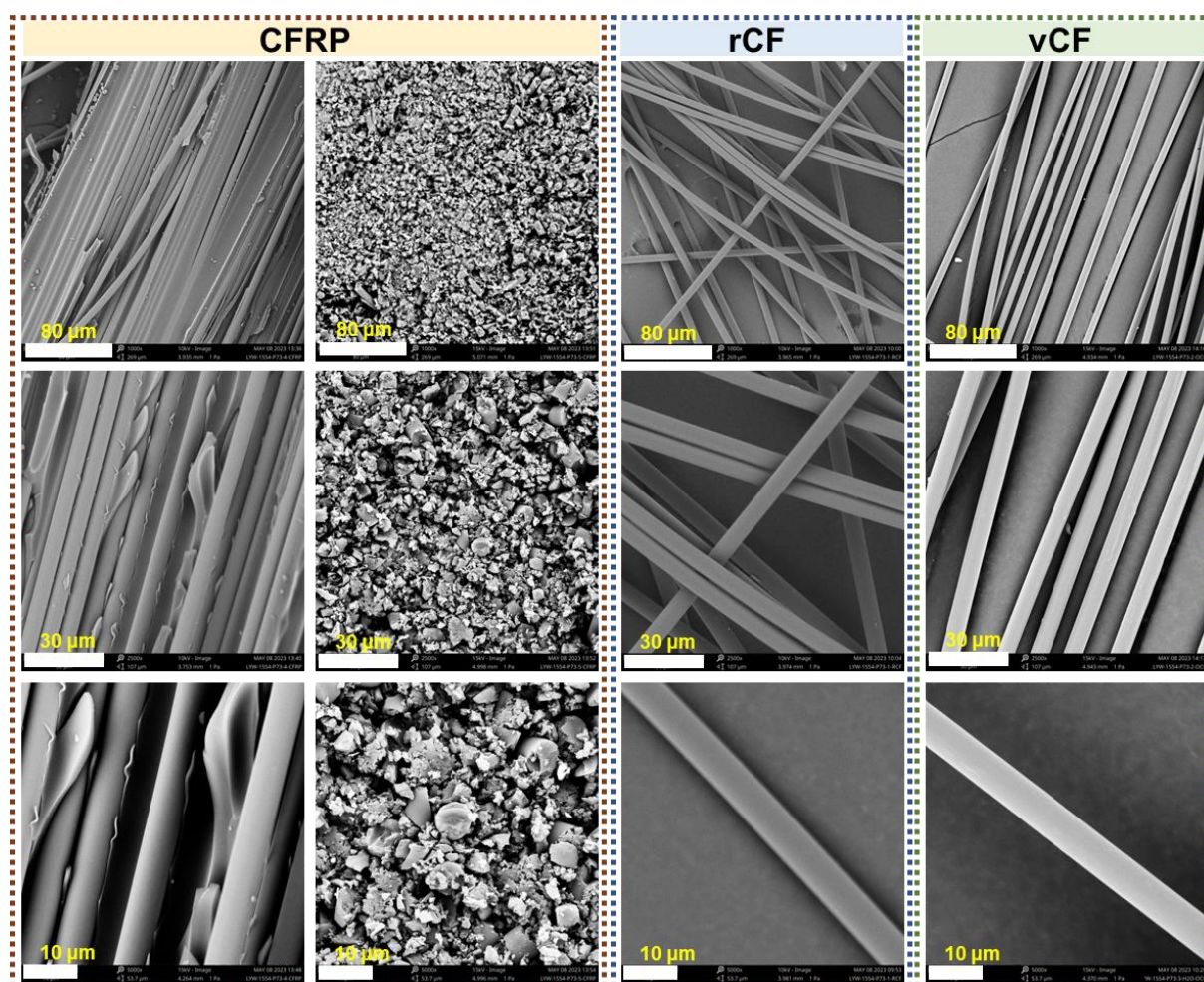

Figure S17. Scanning electron micrographs of CFRP, recovered carbon fibers (rCF) and virgin carbon fibers (vCF)
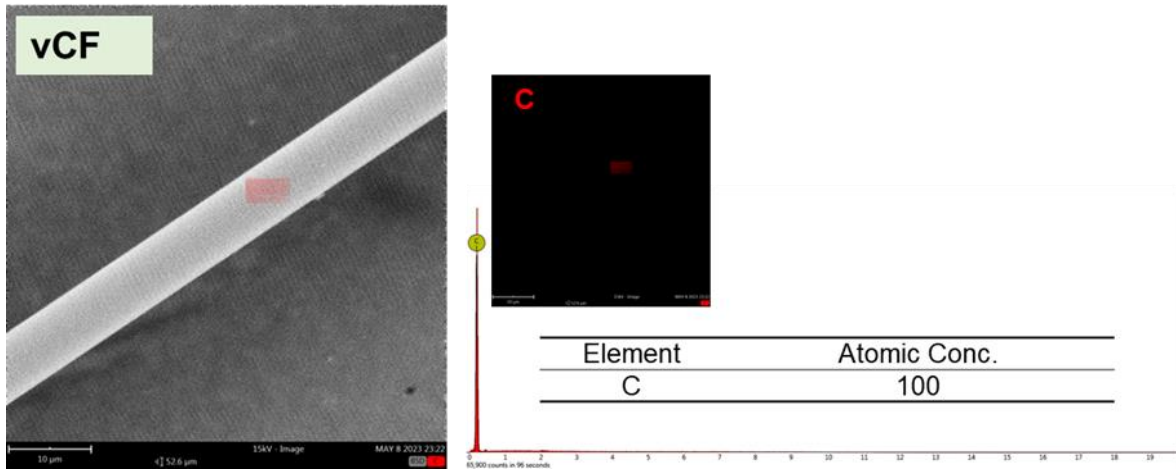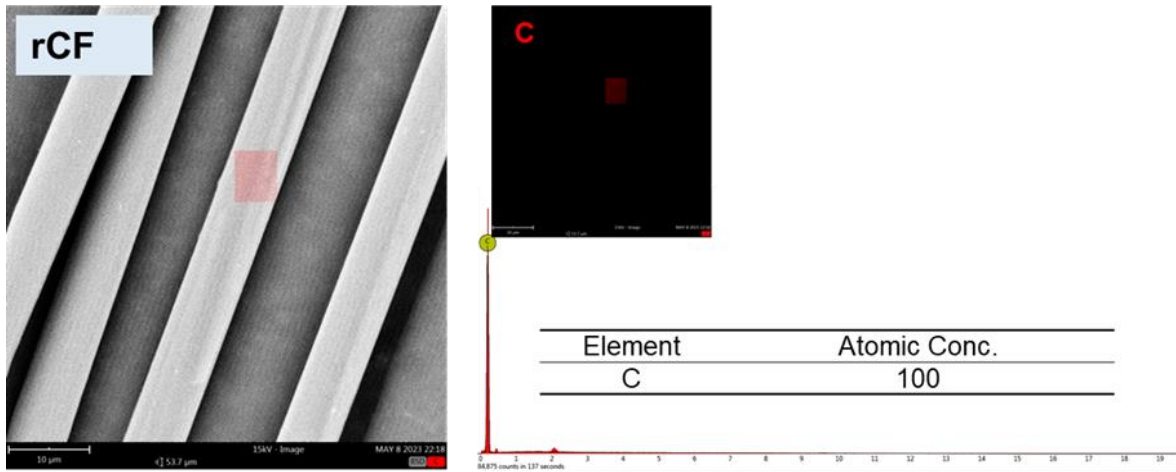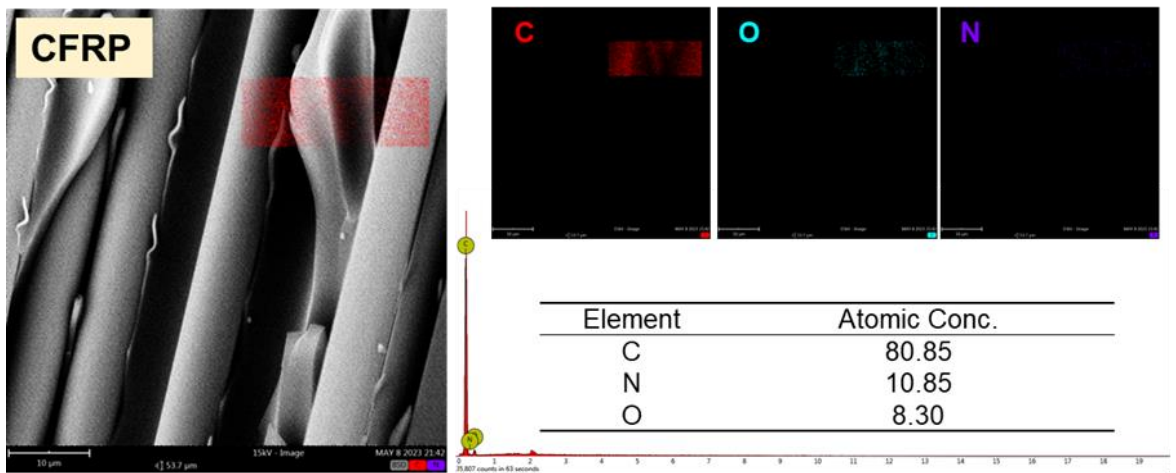
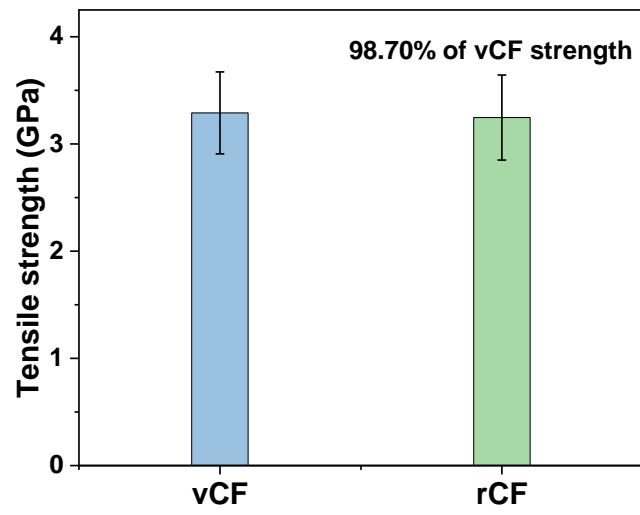**Figure S18.** Scanning electron micrographs and EDS result of CFRP, rCF and vCF

Figure S19. Tensile strength of vCF and rCF

Table S6 The degradation of EP and CFRP

Sample	Substrate	Solution	Temperature (°C)	Time (h)	Degradation rate (%)
1	EP			1	31.33%
2	EP	CAN-H_2O-50%CH_3CN	60	3	47.84%
3	CFRP			1	70.51%
4	CFRP			3	100.00%

Table S7. Comparison of the solvent density at equilibrium state in MD simulation with the experimental results.

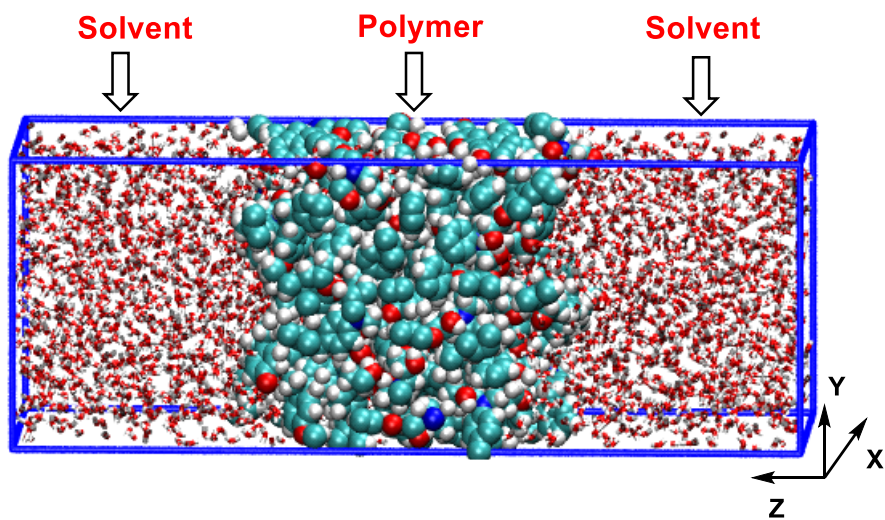| Solvent	Density(g/cm^3)	
	Exp.	Calc.
Water	1.00	0.99
CH$_3$CN	0.79	0.74
H$_2$O-50%CH$_3$CN	0.89	0.91
THF	0.88	0.87
H$_2$O-50%THF	0.94	0.96
DMF	0.94	0.98
H$_2$O-50%DMF	0.97	0.95

Figure S20. Initial swelling model in water solvent in MD simulation as representative.
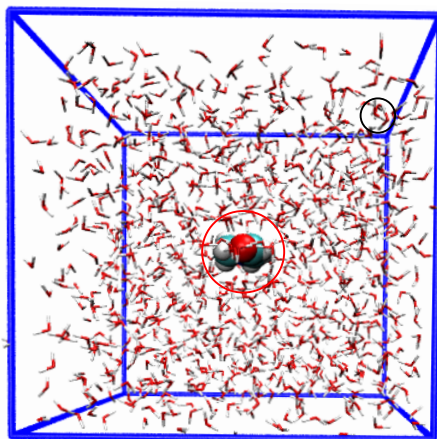
Figure S21. Initial model with one organic molecule (DMF) and water clusters in MD simulation as representative.

References

[1] M. J. Abraham, T. Murtola, R. Schulz, S. Páll, J. C. Smith, B. Hess, E. Lindahl. GROMACS: High performance molecular simulations through multi-level parallelism from laptops to supercomputers. SoftwareX 1 (2015) pp. 19-25.

[2] Y. Zhao and D. G. Truhlar, "The M06 suite of density functionals for main group thermochemistry, thermochemical kinetics, noncovalent interactions, excited states, and transition elements: two new functionals and systematic testing of four M06-class functionals and 12 other functionals," *Theor. Chem. Acc.* 2008, 120, 215-41.

[3] P. C, Hariharan; J. A,Pople. Accuracy of AH Nequilibrium Geometries by Single Determinant Molecular Orbital Theory. *Molecular Physics*, 1974, 27 (1), 209-214.

[4] G. A. Petersson, Andrew Bennett, Thomas G. Tensfeldt, Mohammad A. AI-Laham, and William A. Shirley; A complete basis set model chemistry. I. The total energies of closed-shell atoms and hydrides of the first-row elements. *J. Chem. Phys.* 1988, 89 (4), 2193-2218.

[5] G. W. T. M.J. Frisch, H.B. Schlegel, G.E. Scuseria, M.A. Robb, J.R. Cheeseman, G. Scalmani, V. Barone, B. Mennucci, G.A. Petersson, H. Nakatsuji, M. Caricato, X. Li, H.P. Hratchian, A.F. Izmaylov, J. Bloino, G. Zheng, J.L. Sonnenberg, M. Hada, M. Ehara, K. Toyota, R. Fukuda, J. Hasegawa, M. Ishida, T. Nakajima, Y. Honda, O. Kitao, H. Nakai, T. Vreven, J.A. Montgomery, J.J.E. Peralta, F. Ogliaro, M. Bearpark, J.J. Heyd, E. Brothers, K.N. Kudin, V.N. Taroverov, T. Keith, R. Kobayashi, J. Normand, K. Raghavachari, A. Rendell, J.C. Burant, S.S. Iyengar, J. Tomasi, M. Cossi, N. Rega, J.M. Millam, M. Klene, J.E. Knox, J.B. Cross, V. Bakken, C. Adamo, J. Jaramillo, R. Gomperts, R.E. Stratmann, O. Yazyev, A. J. Austin, R. Cammi, C. Pomelli, J. W. Ochterski, R.L. Martin, K. Morokuma, V.G. Zakrzewski, G.A. Voth, P. Salvador, J.J. Dannenberg, S. Dapprich, A.D. Daniels, O. Farkas, J.B. Foresman, J.V. Ortiz, J. Cioslowski, D.J. Fox, Gaussian 09 (Revision D.01), I. Gaussian, Wallingford, CT, 2013., Gauss.

[6] C. I. Bayly, P. Cieplak, W.D. Cornell, P.A. Kollman, A well-behaved electrostatic potential based method using charge restraints for deriving atomic charges: the RESP model, *J. Phys. Chem.* 1993, 97, 10269-10280.

[7] T. Lu, F. W. Chen, Multiwfn: a multifunctional wavefunction analyzer, *J. Comput. Chem.* 2012, 33, 580-592.

[8] L. Martínez, R. Andrade, E. G. Birgin, J. M. Martínez. Packmol: A package for building initial configurations for molecular dynamics simulations. *J.Comput. Chem.* 30(13):2157-2164, 2009.

[9] J. Wang, R. M. Wolf, J. W. Caldwell, P. A. Kollman, D. A. Case. Development and testing of a general amber force field. *J. Comput. Chem.* 2004, 25, 1157.

[10] H. J. C. Berendsen, J. R. Grigera, and T. P. Straatsma. The missing term in effective pair potentials. *J. Phys. Chem.* 1987, 91, 24, 6269–6271.

[11] P. Wu, R. Chaudret, X. Hu, and W. Yang. Noncovalent Interaction Analysis in Fluctuating Environments. *J. Chem. Theory Comput.* 2013, 9, 5, 2226–2234